

# Progress and Outlook in Monte Carlo Simulations

## 1. Introduction

In 1953, Metropolis et al.<sup>1</sup> introduced an ingenious stochastic method for sampling points in a multidimensional space, according to a prescribed probability distribution defined on that space. One of the great intellectual achievements of the 20th century, Metropolis Monte Carlo has found application in a wide range of scientific and engineering fields. Here, we are mainly concerned with the prediction of thermodynamic properties based on the principles of statistical mechanics. The multidimensional space sampled is the configuration space, spanned by the (generalized) coordinates of the molecules constituting the system plus possibly a few macroscopic extensive variables that are allowed to fluctuate, and the probability density  $\rho^{\text{eq}}$  is set by an equilibrium ensemble. Sampled configuration-space points, or “states,” form a Markov chain, with each state being formed from the previous one in a Monte Carlo (MC) step. In the original MR<sup>2</sup>T<sup>2</sup> algorithm,<sup>1</sup> each MC step is executed in two stages. One first attempts an elementary move from the current state  $i$  into a new state  $j$  with probability  $\alpha(i \rightarrow j)$ , where the stochastic matrix of attempt probabilities is symmetric, satisfying the condition

$$\alpha(i \rightarrow j) = \alpha(j \rightarrow i) \quad (1)$$

One then accepts the attempted move with probability

$$P_{\text{accept}}(i \rightarrow j) = \min \left[ 1, \frac{\rho^{\text{eq}}(j)}{\rho^{\text{eq}}(i)} \right] \quad (2)$$

If the move is rejected, state  $i$  is retained for the current step. With these choices, the transition probabilities  $P(i \rightarrow j) = \alpha(i \rightarrow j) P_{\text{accept}}(i \rightarrow j)$  from state  $i$  to state  $j$  ( $i \neq j$ ) in one step satisfy the condition of microscopic reversibility, or detailed balance,

$$\rho^{\text{eq}}(i)P(i \rightarrow j) = \rho^{\text{eq}}(j)P(j \rightarrow i) \quad (3)$$

As a consequence, the generated Markov chain of states asymptotically samples<sup>2</sup> the probability distribution  $\rho^{\text{eq}}$ . That is to say, in the production phase of a MC simulation, where all configuration-dependent properties fluctuate around constant average values representative of thermodynamic equilibrium, each state  $i$  is sampled with a frequency proportional to its equilibrium probability density  $\rho^{\text{eq}}(i)$ . This is called “importance sampling”.

Originally developed to sample the canonical ( $NVT$ ) ensemble, Metropolis Monte Carlo was readily extended to the isothermal–isobaric ( $NpT$ ) and grand canonical ( $\mu VT$ ) ensembles.<sup>2,3</sup> Moreover, “smart” schemes that use a nonsymmetric matrix of attempt probabilities (i.e., satisfying eq 3 but not eq 1) have been employed to enhance sampling efficiency.<sup>2</sup>

Despite the fact that it cannot provide direct dynamical information, MC has survived as an indispensable molecular simulation tool. Some reasons for this are given as follows:

(a) It can be adapted readily to sample the probability density of new equilibrium ensembles, judiciously designed to address specific systems and problems.

(b) Through creative design of moves that take large strides in configuration space, it can achieve equilibration many orders of magnitude faster than molecular dynamics (MD).

(c) It offers the possibility of introducing rigorous bias schemes, or even dispensing with importance sampling altogether, in addressing the thermodynamics of systems with rugged potential energy hypersurfaces.

Since its early days, MC has been instrumental in testing statistical mechanical theories. Today, it is viewed as a predictive/design tool in its own right. It is capable of providing quantitative or semiquantitative predictions for the composition and structure, thermodynamic properties, phase diagrams, and free energies of systems of immediate technological interest, based on detailed or coarse-grained molecular models. Implemented in the framework of transition-state theory, it can provide estimates of rate constants for infrequent events. As a Kinetic Monte Carlo (KMC) method, it can sample long sequences of such events and thereby track the long-time evolution of diffusion and relaxation processes. It plays a prominent role as part of multiscale modeling/ simulation schemes that bridge the gap between molecular-level interactions and macroscopic properties.

In this article, we briefly review some advances in MC methods over the last 25 years, with an emphasis on contributions made by chemical engineers. In our examples, we will discuss the following: insights obtained from MC simulations concerning separations in complex fluid systems, the processing properties of molten polymers, the sorption capacity and selectivity of nanoporous materials toward industrial gases, and physicochemical characteristics of biological macromolecules. The treatment is necessarily brief and tinted by the author’s own research interests. The author wishes to apologize in advance for not having included some very important pieces of work in this short review.

The article is organized as follows. Section 2 reminds the reader of the significant role played by MC simulation as a tool for testing statistical mechanical theories. Section 3 reviews new ensembles that have been introduced for the prediction of properties, as well as phase and chemical equilibria. Section 4 focuses on new MC moves that have been devised for the efficient sampling of systems with rugged energy hypersurfaces. In section 5, the use of MC for the calculation of free-energy differences and potentials of mean force, with respect to selected slowly evolving degrees of freedom, or “order parameters”, is reviewed. Special techniques for the prediction of phase equilibria close to critical points are discussed in section 6. Section 7 focuses on bold sampling techniques that dispense with importance sampling altogether, with an emphasis on the density-of-states methods. The use of MC sampling and KMC in understanding and predicting long-time dynamics in systems evolving through sequences of infrequent transitions in configuration space is discussed in section 8. A summary and outlook are given in section 9.

## 2. Testing Statistical Mechanical Theories

Since their early days, MC, along with MD simulations,<sup>4</sup> have been valuable as tools for testing statistical-mechanics-based theories for the properties of matter. Comparing theoretical

\* E-mail: doros@central.ntua.gr.

predictions against molecular simulation results based on the same molecular model allows for a direct test of the simplifying assumptions and mathematical approximations invoked in the theory.<sup>2</sup> Moreover, simulations can readily be conducted under extreme conditions of temperature, pressure, and concentration that may be very difficult or costly to attain experimentally.

Chemical engineers have been very active in developing and testing statistical mechanics-based theories for the equation-of-state properties of fluids. A characteristic early example is provided by the work of Dickman and Hall<sup>5</sup> on fluids of chain molecules. They considered fluids of  $n$ -mer chains made of tangent hard spheres of diameter  $\sigma$  with  $n = 4, 8,$  and  $16$  and computed the generalized compressibility factor  $Z^*$ , which is given as

$$Z^* = \frac{1}{n} \left( \frac{p}{\rho k_B T} - 1 \right)$$

with  $T$  being the absolute temperature,  $p$  the pressure,  $\rho$  the molecular density, and  $k_B$  the Boltzmann's constant, as a function of the packing fraction  $\eta$  (given as  $\eta = n\rho(\pi\sigma^3)/6$ ), over a wide range of densities. Comparing predictions from the Wertheim theory and their own generalized Flory theory against MC simulation results, they found very favorable agreement. Moreover, they proposed an ingeniously simple method for obtaining the pressure from the equilibrium density profile adopted by these hard systems in MC simulations between hard repulsive walls. More recently, the statistical associating fluid theory (SAFT), in its various flavors,<sup>6</sup> based on Wertheim's ideas, has been gaining ground as an equation-of-state approach for a wide variety of fluid systems. MC simulations have played a significant role in its development. An excellent illustration of the ways in which Monte Carlo simulation has been used to test and improve molecular-based theories of liquid mixtures for engineering applications is provided in the companion review article by Gubbins and Moore.<sup>7</sup>

Chemical engineers have been very active also in the development of theoretical approaches for fluids sorbed in porous media. An early example is provided by the study of Peterson and Gubbins,<sup>8</sup> who explored phase transitions of a Lennard-Jones (LJ) fluid in an attractive cylindrical pore made up of LJ particles. Figure 1 reproduces some important results of this study. The collision diameter ( $\sigma_w$ ) and well depth ( $\epsilon_w$ ) for LJ interactions between fluid and wall particles were related to the corresponding parameters  $\sigma$  and  $\epsilon$  for fluid–fluid interactions as  $\sigma_w/\sigma = 1.094$ ,  $\epsilon_w/\epsilon = 1.277$ . The number density of particles in the wall was given as  $\rho_w\sigma^3 = 0.988$ . Fluid–fluid interactions were cut and shifted at  $2.5\sigma$ . The inner radius  $R$  of the pore was equal to  $5\sigma$ . Sorption/desorption isotherms for the LJ fluid in the pore are shown at two temperatures:  $0.631T_c$  and  $0.901T_c$ , where  $T_c$  is the gas–liquid critical temperature of the fluid in the bulk. Predictions from application of the local density functional theory of Evans et al.<sup>9</sup> (denoted as Figures 1a and 1c) are compared to grand canonical MC simulation results (denoted as Figures 1b and 1d). Despite some quantitative differences, because of the approximations invoked in the density functional theory, the qualitative behavior is very similar between theory and simulation. At the lower temperature ( $0.631T_c$ ), both theory and simulation predict a first-order transition corresponding to capillary condensation in the pore; the isotherm exhibits two branches with metastable states and hysteresis. At the higher temperature ( $0.901T_c$ ), both theory and simulation predict a continuous isotherm with no phase transition and no hysteresis. Clearly, the isotherms at  $0.901T_c$  are above the critical temperature for capillary condensation, indicating

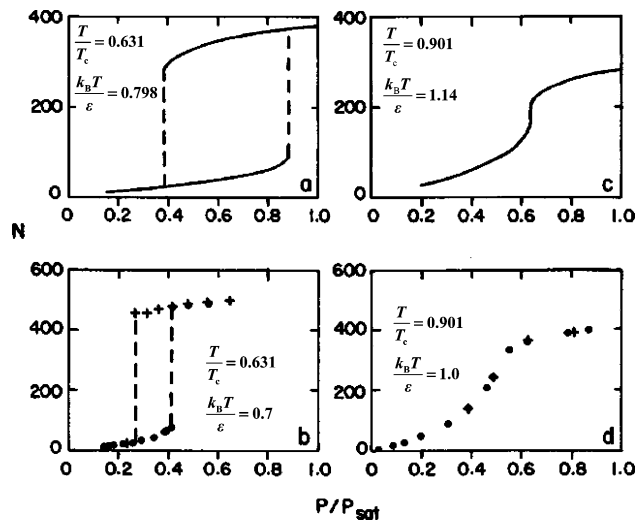


**Figure 1.** Sorption isotherms of a LJ fluid in a cylindrical pore composed of LJ particles at temperatures equal to (a, b)  $0.631$  and (c, d)  $0.901$  times the critical temperature ( $T_c$ ) for the liquid-to-gas transition of the bulk fluid, as obtained by Peterson and Gubbins.<sup>8</sup> The number of fluid molecules  $N$  in a pore is plotted as a function of the pressure (reduced by the saturation pressure at each temperature,  $p/p_{\text{sat}}$ ). Predictions from density functional theory are shown as continuous curves in the top two graphs (panels (a) and (c)), while results from grand canonical Monte Carlo simulations are given as points in the bottom two graphs (panels (b) and (d)).

that the critical temperature for capillary condensation in the pore is significantly below the bulk critical temperature of the fluid ( $T_c$ ).

### 3. New Ensembles

The invention of new ensembles particularly suited for specific systems and properties has greatly enhanced our ability to understand and predict macroscopic thermodynamics based on molecular-level information. Once the probability density ( $\rho^{\text{eq}}$ ) has been derived as a function of the microscopic degrees of freedom, the ensemble can readily be sampled by MC.

An excellent example of a new ensemble invented by a chemical engineer is the Gibbs Ensemble of A. Z. Panagiotopoulos.<sup>10</sup> This ensemble describes two coexisting fluid phases at equilibrium, in the absence of an interface. In its original formulation, applicable to single and multicomponent systems, the total number of particles and the total volume of the two phases are constant, but the volume and the number of particles in each phase are allowed to fluctuate, to ensure an equality of pressures and chemical potentials between the phases. These fluctuations are sampled in the MC through volume and particle exchange moves between the two simulation boxes representing the coexisting phases, which are implemented along with more-conventional moves that displace, rotate, or change the internal configuration of individual molecules in each box. A constant-pressure version of the algorithm, in which the volumes of the two boxes fluctuate independently, has also been developed for multicomponent systems. Gibbs Ensemble MC has been applied very broadly for the calculation of phase equilibria in diverse fluid systems; reviews are available.<sup>11</sup>

A related ensemble is the osmotic ensemble,<sup>12</sup> in which one component is not exchanged between the two coexisting phases; this is well-suited for the prediction of osmotic phase equilibria.

In many applications, one may have a gas phase of given composition, consisting of components  $2, 3, \dots, c$ , in which the component fugacities  $f_2, f_3, \dots, f_c$  can readily be calculated from an equation of state, in equilibrium with a compressible

condensed phase whose main component (component 1) is practically involatile (e.g., a high-molar mass polymer). The solubilities of components 2, 3, ...,  $c$  in the condensed phase and the swelling of that phase as a consequence of sorption can be conveniently predicted through MC simulations of the condensed phase in the  $N_{f2...fcpT}$  ensemble.<sup>13</sup> This is essentially a hybrid between grand canonical and isothermal–isobaric ensembles, in which the pressure, the temperature, the number of molecules of component 1, and the fugacities of components 2, 3, ...,  $c$  are fixed. It is preferable to Gibbs Ensemble MC in the case of an involatile component 1, because it does not require simulation of the gas phase.

Another new ensemble that is very useful for sampling composition fluctuations in binary and multicomponent systems is the semigrand canonical ensemble. This is especially valuable in cases where the molecular insertions/deletions required by grand canonical and Gibbs ensembles and by the Widom test particle insertion method for the chemical potential<sup>2,3</sup> have a low probability of acceptance, because of high density, large molecular size, or strong and specific interactions between molecules. Semigrand ensemble MC equilibrates composition through interconversion moves between species, subject to a prescribed chemical potential difference between the species. Its development has been described well by Briano and Glandt<sup>14</sup> and Kofke and Glandt.<sup>15</sup> A semigrand formulation enabling the simulation of long-chain polymer melts with prescribed molar mass distribution has been presented by Pant and Theodorou.<sup>16</sup>

Reaction ensemble Monte Carlo (RxMC), which allows the simulation of chemically reactive systems at equilibrium, has been a very important development. In 1994, the method was invented independently by Johnson, Panagiotopoulos, and Gubbins<sup>17</sup> and by Smith and Trřska.<sup>18</sup> A comprehensive review was published recently.<sup>19</sup> RxMC uses Monte Carlo sampling to simulate complete forward and reverse chemical reaction events, yielding the equilibrium composition of a reacting mixture. To mimic chemical reactions, RxMC removes reactant molecules from the simulation cell, while product molecules are simultaneously inserted into the cell. The acceptance criterion for such a move must incorporate the free-energy change associated with the attempted chemical conversion in an ideal gas state, plus the change in the energy of physical interactions associated with the removal of reactants and the insertion of products. Inputs to a RxMC simulation are the set of reactions to be simulated; internal molecular partition functions for the reactants and products in the ideal gas state, including vibrational, rotational, and electronic contributions; and a set of intermolecular potentials describing interactions among reactants, products, and any environment in which the reaction takes place, such as the walls of a porous medium. The internal molecular partition functions for isolated molecules are directly related to standard chemical potentials available in compilations of thermochemical data, which are combined to obtain reaction equilibrium constants. RxMC does not require reactive potentials that mimic bond breaking or forming. It is not limited by the rates of the reactions occurring and, using the chemical interconversion moves previously mentioned, it can reach chemical equilibrium very quickly. The combination with Gibbs Ensemble MC has allowed the study of simultaneous phase and reaction equilibria. The method can be used to assess the effects of intermolecular interactions, or the effects of confinement in microporous media, on the equilibrium composition of reacting mixtures. In ref 19, one can find a range of applications of RxMC, including prediction of the equilibrium composition and heat capacity of an argon plasma at 10 bar

and temperatures in the range of  $10^4$ – $10^5$  K. An interesting extension is Transition-State RxMC,<sup>20</sup> in which transition-state species (activated complexes) are introduced as additional chemical species assumed to be at equilibrium with reactants and products, and shifts in chemical reaction kinetics due to environmental effects (e.g., confinement in carbon micropores) are assessed.

In expanded ensemble simulations, one samples a partition function of the form

$$Q_{\text{exp}} = \sum_{i=1}^M Q(y_i) \exp(\psi_{y_i})$$

where  $y$  is a parameter in the system's Hamiltonian, which is allowed to range over  $M$  discrete values or "states".  $Q(y)$  is the partition function at parameter value  $y$ , and  $\exp(\psi_y)$  is a weighting factor that is dependent on  $y$ . Usually,  $y$  governs the coupling of a "tagged" molecule with the rest of the molecules in the system. Moves that change the value of  $y$  are included in the simulation, and a histogram of  $y$  values sampled is maintained. The weights  $\psi_y$  are updated periodically during the course of the simulation, until the  $y$ -histogram becomes flat. At this point, differences in the  $\psi_y$  values provide estimates of the free-energy differences between thermodynamic states corresponding to different  $y$  values. The expanded ensemble method was originally proposed by Lyubartsev et al.<sup>21</sup> and applied to the calculation of the free energy of a primitive model of an electrolyte. In this case,  $y$  was a parameter that modulated ion–ion interactions. As  $y$  decreased from a maximum value to zero, ions were converted from charged hard spheres to uncharged hard spheres, to penetrable hard spheres, to phantom particles. The Helmholtz energy, relative to the ideal gas, was calculated from the histogram of  $y$  values and the profile of imposed  $\psi_y$ . Expanded ensemble MC has been adapted for the calculation of chemical potentials of polymers with  $y$  modulating the length of a "tagged" chain, which is allowed to fluctuate in size.<sup>22,23</sup> More recently, it has been combined with parallel tempering in the so-called "hyperparallel tempering" schemes.<sup>24</sup> Figure 2a presents some results from expanded grand canonical MC simulations of the phase diagram of polymer solutions conducted by Yan and de Pablo, using a simple lattice model (lines).<sup>25</sup> The MC binodals computed for various chain lengths (lines) bear a striking resemblance to the highly asymmetric binodals obtained experimentally in the system polystyrene/methylcyclohexane. From such calculations, one can extract the dependence of the critical volume fraction  $\phi_c$  on chain length. As seen in Figure 2b, a scaling dependence of the form  $\phi_c \approx n^{-0.5}$  is obtained for large chain lengths from a variety of MC simulations with different coarse-grained models.

In parallel tempering (PT) methods, the partition function sampled is a product of partition functions of the system under study, corresponding to different temperatures:  $Q_{\text{PT}} = \prod_{i=1}^M Q(T_i)$ . The temperature levels  $T_i$  are chosen to ensure sufficient overlap between the energy histograms, corresponding to successive  $T_i$  values. In addition to ordinary moves sampling  $Q(T_i)$  at each temperature, a PT simulation employs moves that swap configurations between different temperatures. These greatly enhance sampling efficiency at the lower temperatures. The origins of PT (or replica exchange) can be traced to a paper by Swendsen and Wang,<sup>26</sup> while the form commonly used today was proposed by Geyer.<sup>27</sup> The method was quickly adopted and improved by chemical engineers, most notably by Michael Deem and his group, who have reviewed its principles and applications in physics, chemistry, biology, engineering, and materials science.<sup>28</sup> Advantages of PT include its ease of

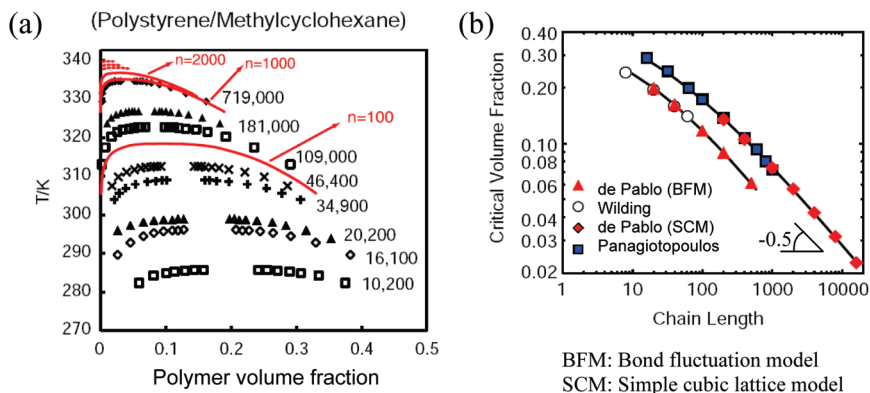


**Figure 2.** (a) Predictions for the liquid–liquid binodal curve in a polymer–solvent system obtained from expanded grand canonical ensemble simulations for various chain lengths  $n$  (lines), compared to experimental binodals from polystyrene–methylcyclohexane systems (points). The numbers next to the experimental binodals indicate the molar mass of the polymer (in  $\text{g mol}^{-1}$ ). (b) Volume fraction of polymer at the liquid–liquid critical point, as a function of the polymer chain length. Results from various calculations with two different lattice-based models are shown. (Reproduced with permission from ref 25. Copyright 2004, Marcel Dekker, New York.)

implementation on top of existing MC or MD codes and its efficient use of multiprocessor computing environments.

A nice example of PT is provided by Falcioni and Deem’s use of the method<sup>29</sup> to determine the structures of zeolites from powder X-ray diffraction (XRD) data. An “energy” function was constructed from bonded geometry and density characteristics of known high-silica zeolites. It was shown that existing, but also new, zeolite types can be discovered as local minima of this energy function with PT. If XRD data are included in the energy function, PT can be used to solve the structure; it clearly outperforms the commonly used, but less rigorous, strategy of simulated annealing. Structures of complex zeolites, including ZSM-5, which contains 12 unique tetrahedral atoms, can be solved with PT.

#### 4. New Moves

Chemical engineers have played a leading role, not only in devising new statistical mechanical ensembles, but also in designing new MC moves for the efficient sampling of complex configuration spaces. Particularly impressive have been advances in the development of new moves for the equilibration of dense polymer systems, which have brought about a virtual renaissance in polymer simulations.

The configurational bias Monte Carlo (CBMC) method was originally proposed by Rosenbluth and Rosenbluth to sample single chains in a lattice.<sup>30</sup> It was reintroduced and placed on a rigorous foundation by Siepmann and Frenkel,<sup>31</sup> as well as by de Pablo, Laso, and Suter.<sup>32</sup> In the CBMC method (see Figure 3a), one cuts away a terminal section of a chain and then regrows it bond by bond, considering several candidate positions for each added skeletal segment. Each time, one of these positions is chosen according to a weight proportional to the Boltzmann factor of the associated change in potential energy. Thus, excluded volume overlaps are avoided during the regrowth procedure and the terminal section is effectively “threaded” through its surroundings. The bias associated with this procedure is taken away by consideration of the inverse move and appropriate design of the selection criteria.

CBMC operates on the ends of chains. To rearrange the conformation of interior segments, a concerted rotation (CONROT) MC method was introduced by Dodd et al.<sup>33</sup> In this move (see Figure 3b), one excises a trimer segment from a random point along the backbone of a randomly chosen chain. One then displaces one or both skeletal atoms flanking the excised trimer by randomly changing one or two “driver” torsion

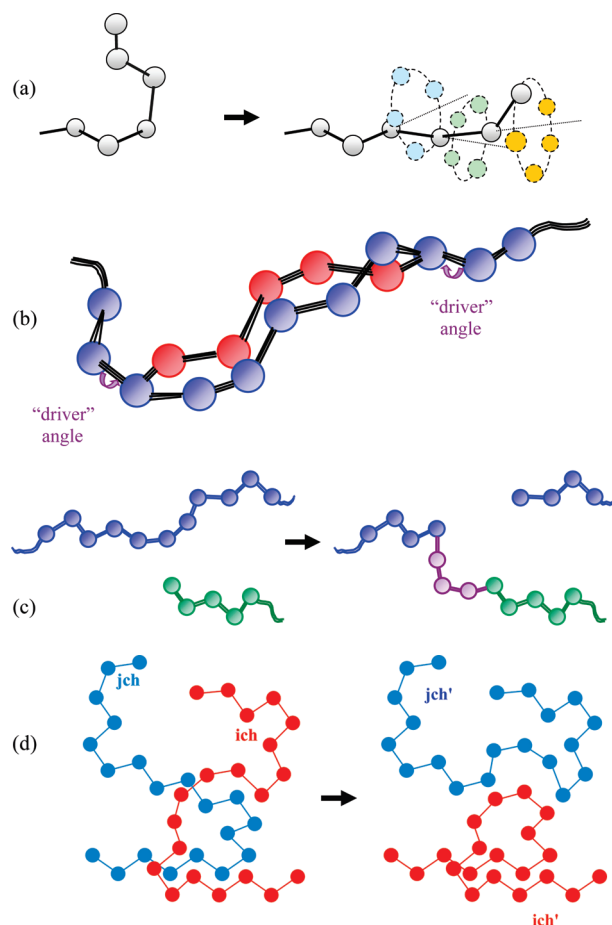


**Figure 3.** Monte Carlo moves for polymers in continuous space: (a) configurational bias, (b) concerted rotation, (c) end bridging, (d) double bridging.

angles, with all preceding and following atoms retaining their positions. The displaced skeletal atoms are finally bridged by construction of a new trimer. The construction of bridging two dimers in space via a trimer, such that the resulting heptamer has prescribed bond lengths and bond angles, is a well-posed geometric problem that admits up to 16 solutions in nondegenerate cases. Many algorithms to solve this problem are available.<sup>33–35</sup> Typically, all solutions are determined and one of them is chosen in a configurationally biased way. Using the trimer bridging construction entails a geometric transformation from atomic Cartesian coordinates to the internal coordinates

that are constrained during bridging; the Jacobian of this transformation in the original and final configurations must be incorporated in the selection criterion.<sup>33,34</sup>

Equilibrating the long-range conformational features of chains (end-to-end distance, radius of gyration) is a major challenge in molecular simulations of long-chain polymer systems. The longest relaxation time of a polymer melt scales with chain length  $n$  as  $n^2$  below the critical chain length for entanglements (Rouse regime) and as  $n^{3.4}$  above it (reptation regime, modified by contour length fluctuations and constraint release). For entangled polymer melts encountered in plastics processing operations, the longest relaxation time is in the range of milliseconds to minutes; thus, equilibrating such a melt, in most situations, is impossible with MD, which can access times up to microseconds on currently available computers.<sup>36</sup> This barrier to the equilibration of long-chain polymer systems has been overcome through the development of connectivity-altering MC moves.<sup>37</sup> These moves can be implemented readily on atomistic models by invoking the trimer bridging construction. In the End-Bridging Monte Carlo (EBMC) method<sup>16,34</sup> (see Figure 3c), the end of a chain attacks the interior of another chain, separating it into two pieces by excision of a trimer segment. Subsequently, the attacking end is connected to one of the two pieces of the victim chain by construction of a new trimer. The move generally changes the lengths of the chains involved. It is implemented, along with reptation and CONROT moves, in a semigrand ensemble formalism, in which the total number of chains, the total number of monomer units, the pressure, the temperature, and the relative chemical potentials of all chain species but two are held constant. One can control the molar mass distribution of the polymer at equilibrium by imposition of an appropriate profile of chemical potentials.<sup>16</sup> A remarkable attribute of the EBMC method is that the CPU time that it requires to equilibrate the end-to-end vectors of chains actually *decreases* with increasing chain length, in sharp contrast to what happens in MD and real melt dynamics.

To equilibrate strictly monodisperse melts, one can employ the double bridging<sup>38</sup> (DB) move (see Figure 3d). Here, one excises two trimer segments from two nearby chains and subsequently builds two trimer bridges, to form two new chains of exactly the same length, but entirely different conformations.

Connectivity-altering moves have been applied to united-atom models of linear and star polyethylene and their blends, of short-chain branched polyethylene, of isotactic, syndiotactic, and isotactic polypropylene, of cis-1,4- and cis-1,2-polybutadiene, of cis-1,4-polyisoprene, and of poly(ethylene oxide) terminated in hydroxyl and methoxy groups. They have also been applied to coarse-grained models of atactic polystyrene and poly(ethylene terephthalate). For the first time, they have enabled the full equilibration of polymer melts well in the entangled regime, with molar mass distributions comparable to those encountered in processing operations. Equilibrated configurations obtained by connectivity-altering MC methods have served as starting points for atomistic studies of dynamics in the Rouse and reptation regimes and for topology-preserving reductions to entanglement networks useful in the mesoscopic analysis of melt flow and large-scale deformation of solid amorphous polymers. Thus, connectivity-altering MC methods play a strategically important role in the prediction of polymer properties through hierarchical and multiscale modeling.<sup>37,39</sup>

Figure 4 reproduces some results on packing and chain dimensions in a series of short-chain branched polyethylenes that consist of backbones of average length  $C_{1000}$  and  $C_4$  branches, as obtained by connectivity-altering MC simulations.<sup>40</sup>

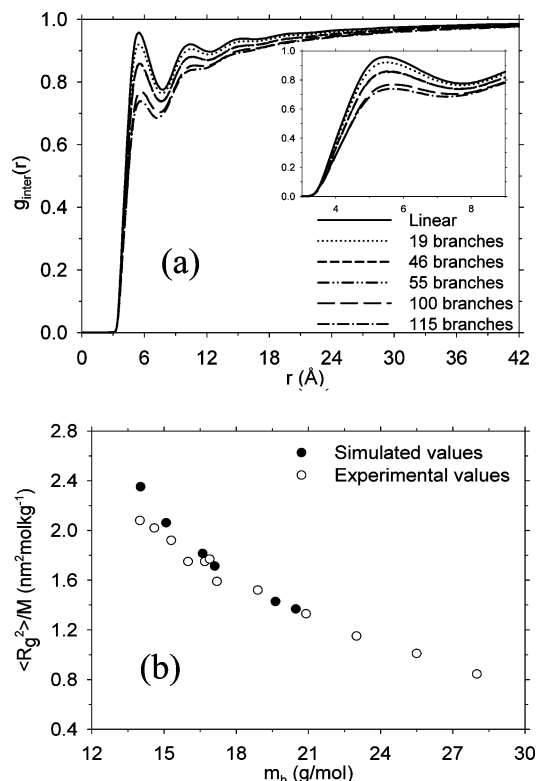


**Figure 4.** (a) Intermolecular pair distribution function and (b) mean square chain radius of gyration divided by molar mass in a series of short-chain branched polyethylene melts (random copolymers of ethylene and 1-hexene) with different degrees of branching at 450 K and 1 bar. In panel (a), curves are labeled according to the number of branches per 1000 backbone carbons. In panel (b), the degree of branching is measured using the average chain molar mass per backbone bond ( $m_b$ ). Experimental values are obtained via small-angle neutron scattering (SANS) analysis on molten ethylene–1-butene copolymers.<sup>40</sup>

The chains are random copolymers of ethylene and 1-hexene and constitute a good model for polyethylenes synthesized via metallocene catalysis. Melts with 0–115 branches per 1000 backbone carbons were simulated at 450 K and 1 bar, using the TraPPE united atom force field, which is known to reproduce the equation-of-state and vapor–liquid equilibrium properties of short alkanes. Figure 4a shows the intermolecular pair distribution function  $g_{inter}(r)$ , which characterizes molecular packing in the simulated melts. As the degree of branching increases, the “correlation hole” effect (suppression of  $g_{inter}(r)$ , relative to 1 at distances smaller than the chain radius of gyration) becomes more pronounced; the location of the first peak, which is indicative of the distance between neighboring chains in the melt, shifts slightly to the right (detail shown in the inset), because more branched chains behave as “fatter” objects. Figure 4b displays changes in the conformational stiffness with the degree of short-chain branching. The ratio  $\langle R_g^2 \rangle / M$  of the mean square radius of gyration to molar mass is used as a measure of conformational stiffness, while the average molar mass per backbone bond ( $m_b$ ) is used as a measure of the degree of branching. Clearly, the introduction of even small degrees of branching reduces conformational stiffness very significantly; this prediction, which can be explained in terms of changes in the backbone torsion angle distribution brought about by short-chain branching,<sup>40</sup> is confirmed by experimental data from small-angle neutron scattering (SANS). The latter, which come from ethylene–1-butene, rather than ethylene–1-hexene copolymer melts, nevertheless follow the trend predicted by simulations almost quantitatively.

## 5. Calculation of Free-Energy Differences

The calculation of free-energy differences is of paramount importance, with regard to understanding and predicting phase equilibria and stability in a wide variety of physicochemical, materials, and biomolecular systems, yet remains a challenging problem for molecular simulation. As discussed in an instructive review by Kofke,<sup>41</sup> methods for the calculation of the Helmholtz energy difference  $A_2 - A_1$  between two systems 1 and 2 fall into two broad categories: density-of-states methods and work-based methods.

In *density of states methods*,  $A_2 - A_1$  is calculated as

$$A_2 - A_1 = -k_B T \ln \left( \frac{P_2}{P_1} \right) \quad (4)$$

where  $P_i$  is the probability of sampling system  $i$  in an equilibrium simulation, which is given complete freedom to explore both systems. In practice, bias techniques may be used to ensure efficient sampling of both systems.

*Work-based methods*, on the other hand, can be envisioned as applications of the Jarzynski equality,<sup>42</sup>

$$A_2 - A_1 = -k_B T \ln \left[ \overline{\exp \left( -\frac{W_{1 \rightarrow 2}}{k_B T} \right)} \right] \quad (5)$$

where  $W_{1 \rightarrow 2}$  is the work associated with a process (not necessarily reversible!) that transforms system 1 into system 2, usually by modulating a parameter in the Hamiltonian of the system, and the overbar denotes averaging over an ensemble of such transformations, beginning from an equilibrated system 1. When the transformation of 1 into 2 occurs reversibly, eq 5 leads to the *thermodynamic integration* method. When, on the other hand, an instantaneous transformation of individual configurations of system 1 into the corresponding configuration of system 2 is undertaken, eq 5 is reduced to the *free energy perturbation* method,

$$A_2 - A_1 = -k_B T \ln \left\langle \exp \left( -\frac{v_2 - v_1}{k_B T} \right) \right\rangle_1 \quad (6)$$

where the ensemble average is taken over all configurations of system 1, distributed according to the canonical ensemble, and  $v_1$  and  $v_2$  denote the potential energy functions of systems 1 and 2, respectively, evaluated at each sampled configuration. For free-energy perturbation to work, the region of configuration space that shapes the properties of system 2 must be a subset of that of system 1. If this is not the case, staging schemes can be invoked.<sup>41</sup>

An early example of free-energy perturbation is Widom's test particle insertion method for the chemical potential.<sup>43</sup> The excess chemical potential is computed as

$$\mu^{\text{ex}}(\rho, T) \equiv \mu(\rho, T) - \mu^{\text{ig}}(\rho, T) = -k_B T \ln \langle \exp(-\beta v_{\text{test}}) \rangle_{\text{Widom}} \quad (7)$$

where  $v_{\text{test}}$  is the energy "felt" by a test particle inserted in the system of real particles and the average is taken over all configurations, sampled according to the canonical ensemble, and over all points of insertion in the simulation box, sampled uniformly. Widom insertion is extremely useful in the calculation of solubilities and fluid-phase equilibria. Unfortunately, it becomes inefficient at high densities and low temperatures, because most random insertions lead to overlap with  $\beta v_{\text{test}} \rightarrow \infty$ . This insertion problem is especially severe for bulky

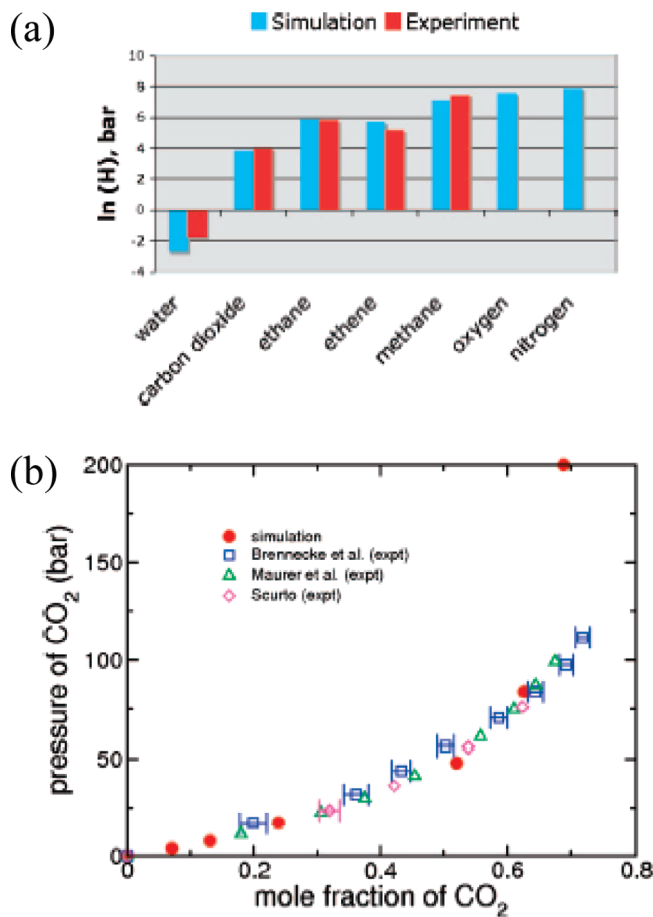


**Figure 5.** (a) Comparison between predicted and experimental Henry's law constants for various gases in the ionic liquid 1-*n*-butyl-3-methyl-imidazolium hexafluorophosphate, [C<sub>4</sub>mim][PF<sub>6</sub>], at 298 K. (b) Predicted sorption isotherm for CO<sub>2</sub> in the ionic liquid 1-*n*-hexyl-3-methyl-imidazolium bis-(trifluoromethylsulfonyl) imidate, [C<sub>6</sub>mim][Tf<sub>2</sub>N], at 333 K. (Reproduced, with permission, from ref 48. Copyright 2007, American Chemical Society, Washington, DC.)

molecules, molecules of complex shape, and molecules that experience strong and specific interactions, such as hydrogen bonding, with their surroundings. Chemical engineers have been active in devising methods to alleviate the insertion problem. For flexible molecules, insertions can be implemented in a configurationally biased way, as proposed by Maginn et al.,<sup>44</sup> for the case of long alkanes in zeolite pores. For bulky molecules, particle deletion (or inverse Widom<sup>45</sup>) methods are useful. In those, one must realize that deleting a molecule from a  $N$ -molecule configuration does not lead to an ordinary configuration of the remaining  $(N - 1)$  molecules, but rather to a  $(N - 1)$ -molecule configuration with a hole in it; the bias associated with the presence of the hole can be rigorously removed. In minimum mapping (minmap) methods,<sup>46</sup> the number of degrees of freedom is adjusted around an inserted molecule to alleviate overlaps and around a deleted molecule to close holes. Shi and Maginn's continuous fractional component MC method<sup>47</sup> is an open-system MC method that employs gradual insertions and deletions of molecules through the use of a continuous coupling parameter, an adaptive bias potential, and hybrid MC for equilibration.

Recently, a fertile domain of application of chemical potential estimation and open-system MC methods has been the computational prediction of solubilities in ionic liquids.<sup>48</sup> Figure 5a shows predictions for the Henry's constants of various small molecules in the ionic liquid 1-*n*-butyl-3-methyl-imidazolium hexafluorophosphate, or [C<sub>4</sub>mim][PF<sub>6</sub>], at 298 K, along with

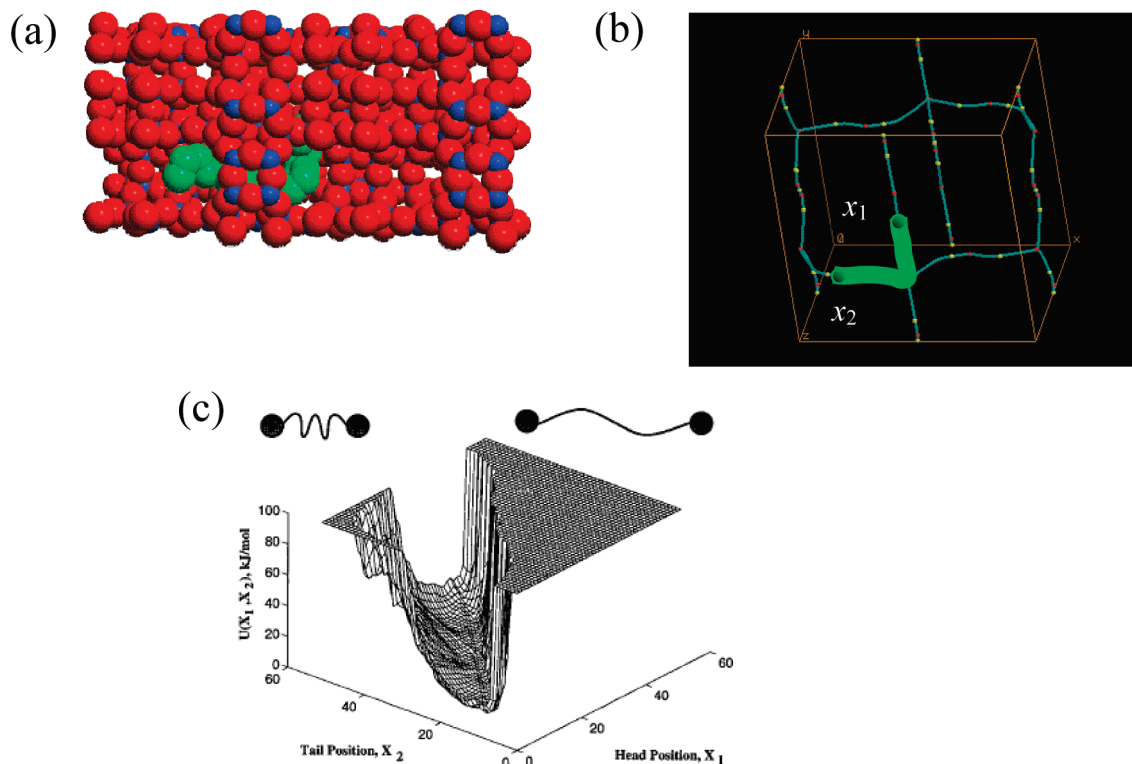


**Figure 6.** (a) Atomistic and (b) coarse-grained representation of an *n*-icosane molecule sorbed in silicalite-1. At the coarse-grained level, the molecule is represented by the sequence of channel segments and intersections it goes through and by the positions  $x_1, x_2$  of its two ends along their respective channels. (c) Potential of mean force  $U(x_1, x_2)$  for an *n*-octane molecule straddling an intersection, with its two ends in straight channel segments.<sup>49</sup> Large (small) values of  $x_1 - x_2$  correspond to extended (compressed) conformations of the molecule inside the channels.

experimental estimates. A full sorption isotherm for CO<sub>2</sub> in the ionic liquid 1-*n*-hexyl-3-methyl-imidazolium bis-(trifluoromethylsulfonyl) imidate, [C<sub>6</sub>mim][Tf<sub>2</sub>N] at 333 K, as determined by simulation and as measured by a variety of groups, is shown in Figure 5b. Up to pressures of 120 bar, simulation predictions are within 10% of the experimental measurements, underlining the promise of MC simulations as tools for the molecular design of separations and chemical reactions, based on these complex solvents.

As a special case of free-energy calculation, we discuss the extraction of *potentials of mean force* from atomistic simulations. This is strategically important in coarse-graining strategies for addressing long time- and length-scale properties. Generally, if we partition the configuration space of a system into a subset of (slowly evolving) degrees of freedom ( $\mathbf{R}$ ), upon which we wish to focus, and a complementary subset of (fast) degrees of freedom ( $\mathbf{r}$ ), we define the potential of mean force with respect to  $\mathbf{R}$ ,  $U(\mathbf{R})$ , as

$$U(\mathbf{R}) = -k_B T \ln \int \exp[-\beta v(\mathbf{R}, \mathbf{r})] d\mathbf{r} + \text{constant} \quad (8)$$

with  $\beta = 1/(k_B T)$ .  $U(\mathbf{R})$  is a configurational free energy that describes effective interactions among the degrees of freedom  $\mathbf{R}$ , assuming that the degrees of freedom  $\mathbf{r}$  are always equilibrated subject to the current values of  $\mathbf{R}$ ; this will be the case if the relaxation times for the motion of  $\mathbf{r}$  are much shorter than the characteristic times governing the evolution of  $\mathbf{R}$ . The potential of mean force provides a correct and consistent thermodynamic description of the degrees of freedom  $\mathbf{R}$ , having projected out  $\mathbf{r}$ . A correct *dynamical* description cast exclusively in terms of the subset  $\mathbf{R}$  generally is much more difficult to formulate. It is provided by Zwanzig and Mori's projection operation formalism,<sup>2</sup> and it is commonly approximated via

Brownian dynamics, Langevin dynamics, dissipative particle dynamics, and related schemes. In all these schemes, the gradient of the potential of mean force must be used as the thermodynamic driving force, to ensure consistency with the full atomistic description.

Efficient MC schemes are valuable in calculating the potentials of mean force  $U(\mathbf{R})$ , with respect to selected coarse-grained degrees of freedom  $\mathbf{R}$ . An early example is provided by the work of Maginn et al. on sorption and diffusion of long linear alkanes in the zeolite silicalite-1.<sup>44,49</sup> As shown pictorially in Figures 6a and 6b, at the coarse-grained level, the zeolite was reduced to a set of intersecting curved lines representing the axes of straight and sinusoidal channels and computed directly from the force field exerted on a test particle inside the zeolite crystal. A sorbed alkane was coarse-grained into a linear wormlike object that is defined by the sequence of channel segments and intersections it goes through and by the positions  $x_1, x_2$  of its two ends along the channel segments in which they find themselves. The potential of mean force  $U(x_1, x_2)$  was computed by CBMC integration. Figure 6c shows the typical shape of the potential of mean force. It refers to an *n*-octane molecule sorbed along a straight channel of silicalite in an extended conformation, in such a way as to straddle a channel intersection. A distinctive characteristic of  $U(x_1, x_2)$  is a low-energy trough, along which  $x_1 - x_2$  is more or less constant. Moving along this trough corresponds to sliding the molecule along the straight channel. The favorable energy it experiences in the trough is due to dispersive interactions with the zeolite lattice. If one tries to extend the contour of the sorbed molecule (increasing  $x_1 - x_2$ ), one encounters a steep repulsive wall, because one must work against intramolecular bending potentials. If one tries to compress the contour of the molecule (decreasing  $x_1 - x_2$ ), the potential of mean force increases again,

because of confinement, but not as steeply as in the case of stretching the molecule. Potentials of mean force, such as that of Figure 6c, were used within a Brownian dynamics/transition state theory formulation to track the intracrystalline diffusion of C<sub>4</sub>–C<sub>20</sub> molecules inside silicalite-1.<sup>49</sup> Predictions were confirmed *a posteriori* via quasielastic neutron scattering measurements.<sup>50</sup>

Direct calculation of a potential of mean force from atomistic simulation in a polymer system is exemplified by the work of Mavrantzas and Theodorou.<sup>51</sup> There, the conformation tensor (dyadic product of the end-to-end vector with itself, averaged over all chains and reduced by one-third of its trace in the equilibrium undeformed state) was employed as a coarse-grained variable in expressing the Helmholtz energy of an unentangled melt under steady-state elongational flow. Results were used to test various dumbbell models invoked in theories of melt viscoelasticity, to obtain the stress tensor as a function of strain rate, and to predict birefringence in the flowing melt.<sup>37</sup>

## 6. Special Techniques for Phase Equilibria and Critical Points

As already mentioned above, the calculation of phase equilibria in fluid systems has received special attention by chemical engineers. Predicting critical points by simulation is especially challenging, because the correlation length for density or composition fluctuations diverges in their vicinity, and, thus, extremely large boxes would be required for adequate sampling of such fluctuations. Here, we briefly discuss some techniques for the calculation of phase equilibria and critical points, which were devised or improved by chemical engineers.

Starting from a known point on the phase coexistence curve (determined, e.g., by the Gibbs Ensemble MC method), Gibbs–Duhem integration<sup>52</sup> allows one to calculate the complete phase diagram through a series of constant  $p$ -calculations that involve no particle transfers. For a one-component system, one integrates the Clapeyron equation,

$$\left(\frac{dp}{d\beta}\right)_{\text{sat}} = -\frac{\Delta H}{\beta\Delta V} \quad (9)$$

moving along the two branches of the binodal curve.

Finite-size scaling is a systematic method for correcting simulation estimates of critical properties for size dependence. For example, the critical temperature  $T_c(L)$  and critical density  $\rho_c(L)$ , obtained from model systems of finite size  $L$ , can be estimated from grand canonical MC simulations and extrapolated to the infinite system size limit, based on the universal form of the normalized probability distribution of an appropriately defined ordering operator (e.g.,  $M = N - sv$ ) at criticality and on the scaling relations expressing  $L$ -dependent deviations from the infinite system limit. The method was proposed by Bruce and Wilding<sup>53</sup> and was applied extensively to complex fluids by Orkoulas and Panagiotopoulos.<sup>54</sup>

Histogram reweighting uses multiple overlapping MC runs under different conditions (e.g., grand canonical MC runs at given  $V$  values under various  $\mu$  and  $T$  values) to accumulate a histogram of the density of states (e.g.,  $\Omega(N, E)$ , which is the number of states with  $N$  molecules and energy  $E$  at volume  $V$ ) with optimal statistical efficiency. From the density of states, one can then calculate thermodynamic properties under different conditions. The method was proposed by Ferrenberg and Swensen,<sup>55</sup> and it was applied to the phase equilibria of chain fluids by the Panagiotopoulos group.<sup>56</sup>

The transition-matrix MC method was advanced to improve sampling in systems with rugged energy hypersurfaces, where

a regular MC simulation may be trapped within subspaces of the configuration space and never access other regions that contribute significantly to thermodynamic properties. In the transition-matrix MC method, one first defines “macrostates” by partitioning into subdomains the domain from which a configurational variable (or a small set of such variables) takes values. For example, one may define macrostates according to the number of molecules  $N$  present in the simulation box in a grand canonical MC run. In the course of the run, one updates a collection matrix with the acceptance probabilities of moves between configurations belonging to different macrostates. By normalizing this collection matrix, one obtains a transition probability matrix between macrostates. From the transition probability matrix, one can estimate the stationary probability distribution among macrostates expected at equilibrium. This probability distribution is used to bias moves in a self-adaptive way, enhancing the sampling of less-probable macrostates. The method arose in the statistical physics community,<sup>57</sup> but it has been developed and used in inventive ways by chemical engineers (most notably, Errington and his group<sup>58</sup>).

## 7. Density of States Methods

Recently, a trend to move away from importance sampling toward schemes that sample configuration space more uniformly can be noted. This is exemplified by the expanded ensemble, parallel tempering, histogram reweighting, and transition-matrix methods discussed above.

In 2001, Wang and Landau<sup>59</sup> introduced a method that dispenses with importance sampling altogether. The Wang–Landau, or the Density of States, method, focused on sampling configurations  $i$  with probability  $P_i \propto 1/(\Omega(v_i))$ , where  $\Omega(v)$ , the “density of states”, is the number of configurations with potential energy  $v$ . If this probability distribution of configurations is realized, the histogram of potential energy values sampled by the algorithm will be uniform. The algorithm attempts a random walk in configuration space. Random moves are accepted or rejected according to the Metropolis-type criterion

$$P_{\text{accept}}(i \rightarrow j) = \min\left[1, \frac{\Omega(v_i)}{\Omega(v_j)}\right] \quad (10)$$

Of course, the density of states  $\Omega(v)$  is not available *a priori*; the algorithm uses a running estimate of it, which is improved as the simulation proceeds. Initially,  $\Omega(v)$  is set equal to 1 throughout. Everytime a new value of  $v$  is visited, the corresponding estimate of  $\Omega(v)$  is updated via  $\Omega(v) \rightarrow f\Omega(v)$ , with  $f$  being a convergence factor. Initially,  $f$  is set equal to the base of natural logarithms ( $e$ ). A histogram  $h(v)$  of potential energy values visited by the simulation is accumulated and checked periodically. When  $h(v)$  is sufficiently flat, the algorithm erases it and starts accumulating it anew, with  $f \rightarrow f^{1/2}$ . The calculation stops when  $f$  is sufficiently close to 1. At this point, detailed balance is essentially satisfied by the scheme of sampling configurations. From  $\Omega(v)$ , all thermodynamic properties of the system can be computed. Significant contributions to the Density of States MC methodology and applications have been made by Shell et al.<sup>60</sup> and by Mastny and de Pablo.<sup>61</sup>

The Density of States MC method has been used successfully to study the phase transitions of individual macromolecules in solution, namely, the coil to globule and crystallization transitions of synthetic polymer chains and protein folding. Figure 7 summarizes some results from a MC study of confinement effects on protein folding by Rathore et al.<sup>62</sup> They employed

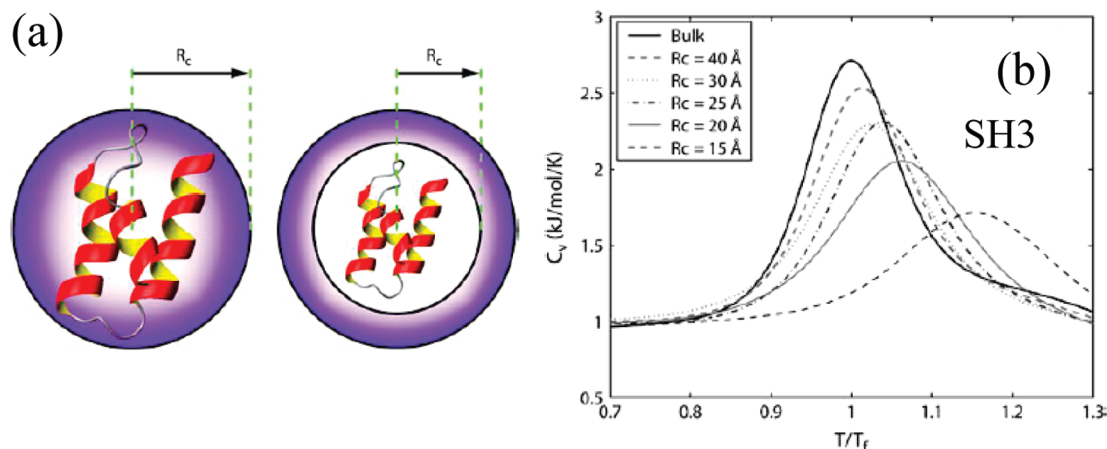


**Figure 7.** (a) Simple models of protein confinement considered by Rathore et al.:<sup>62</sup> (left) soft repulsive cavity and (right) hard cavity. (b) Heat capacity of a SH3 protein in a hard cavity, as a function of temperature, as computed from Density of States MC simulations, for various confinement radii  $R_c$ .  $T_f$  is the “melting” temperature of the free protein in solution ( $T_f = 378.9$  K).

minimalist coarse-grained models with  $G\bar{o}$ -type interactions for the proteins and simple spherically symmetric potentials to mimic confinement in a chaperonin cage. Two types of confining potentials were considered: a soft repulsive one and a hard one, depicted schematically in Figure 7a. The question that was addressed was this: how does the folding, and its opposite “melting” transition, of the protein depend on the confining potential and the confinement radius? From the Density of States MC method, one can readily compute the heat capacity, based on the fluctuation of energy at constant temperature. If one categorizes the sampled conformations into “folded” and “unfolded”, according to the number of native contacts present, one can also compute differences in Gibbs energy, enthalpy, and entropy between folded and unfolded structures. Figure 7b shows the heat capacity as a function of temperature for a SH3 protein subject to a hard confining potential, for various confining radii  $R_c$ . The transition temperature, taken as the temperature where a maximum in the heat-capacity curve is observed, moves to higher values, indicating that the folded structure is stabilized upon confinement. At the same time, the transition becomes broader for the confined protein. The effect of confinement on the transition was determined to be dependent on the protein and on the form of the confining potential, and it was observed to be nonmonotonic with respect to  $R_c$  in some cases.<sup>62</sup>

## 8. Monte Carlo as a Tool for Understanding and Predicting Long-Time Dynamics

One typically thinks of MC simulations as a family of stochastic methods for understanding and predicting the equilibrium properties of matter. In addition, however, MC simulations represent a valuable tool for addressing dynamical properties. This is especially true for physical, chemical, materials, and biological systems whose dynamics proceeds as a sequence of infrequent transitions between low-energy basins, or “states”, in configuration space. In such systems, the mean waiting time for a transition out of a state is long, in comparison to the time required for the system to establish a restricted equilibrium distribution among configurations in the state (time scale separation). Examples of phenomena that occur as successions of infrequent events include the following: diffusion in solids, in nanoporous materials, and in amorphous polymers; surface diffusion; protein folding; structural relaxation and plastic deformation of glassy materials; chemical and biochemi-

cal reactions; breakup and coalescence phenomena in emulsions and foams; and phase transitions in molecular and atomic clusters.

A coarse-grained description of the dynamics of such phenomena is provided by a master equation,

$$\frac{\partial P_i(t)}{\partial t} = \sum_{j \neq i} P_j(t) k_{j \rightarrow i} - P_i(t) \sum_{j \neq i} k_{i \rightarrow j} \quad (11)$$

where  $P_i(t)$  is the probability of residing in state  $i$  at time  $t$  and  $k_{i \rightarrow j}$  is a rate constant (transition probability per unit time) for transitions from state  $i$  to state  $j$  (see Figure 8). MC methods are valuable (i) with regard to estimating the rate constants  $k_{i \rightarrow j}$  from the atomistic potential energy hypersurface of the system and the atomic masses, and (b) with regard to solving the master equation numerically, and thereby tracking the long-time temporal evolution of the system. Both of these aspects are strategically important, because, in many systems, the characteristic times that govern the properties of interest are much longer than microseconds and, therefore, cannot be addressed reliably with MD.

The theory of infrequent events<sup>63</sup> provides a framework for calculating rate constants  $k_{i \rightarrow j}$  from the potential energy hypersurface of the system and atomic masses. Transition-state theory (TST) postulates that any trajectory that crosses the dividing surface between states  $i$  and  $j$  will effect a successful transition between states  $i$  and  $j$ . With this assumption, the rate constant can be obtained as

$$k_{i \rightarrow j}^{\text{TST}} = \frac{k_B T Q^\ddagger}{h Q_i} = \frac{k_B T}{h} \exp\left(-\frac{G^\ddagger - G_i}{k_B T}\right) \quad (12)$$

where  $h$  is Planck’s constant;  $Q^\ddagger$  and  $G^\ddagger$  are the isothermal–isobaric partition function and the Gibbs energy of the system confined to the dividing surface, respectively; whereas  $Q_i$  and  $G_i$  are the isothermal–isobaric partition function and the Gibbs energy of the system over the entire origin state  $i$ . Note that the dimensionality of the system described by  $Q^\ddagger$  and  $G^\ddagger$  is, by one, less than that described by  $Q_i$  and  $G_i$ .

Figure 9a gives a simple geometric representation of states and the dividing surface for a system with three degrees of freedom. It can be thought of as corresponding to a spherical molecule jumping between two cavities within an inflexible porous medium, such as a zeolite. For this simple case, eq 12 can be reduced to

$$k_{i \rightarrow j}^{\text{TST}} = \left( \frac{k_B T}{2\pi m} \right)^{1/2} \frac{\int_{\text{bottleneck surface}} \exp\left(-\frac{v(\mathbf{r})}{k_B T}\right) d^2 r}{\int_{\text{state } i \text{ volume}} \exp\left(-\frac{v(\mathbf{r})}{k_B T}\right) d^3 r} \quad (13)$$

where  $v(\mathbf{r})$  is the potential energy, as a function of position  $\mathbf{r}$  of the molecule in the medium, and  $m$  is the mass of the molecule. The configurational integrals can be computed via MC integration.<sup>64</sup> Alternatively, the ratio of configurational integrals can be computed by free-energy perturbation.

TST is not exact. In reality, the trajectory may recross the dividing surface, ultimately thermalizing in the origin state. There may even be fast multistate transitions, wherein the system traverses state  $j$  quickly and ultimately thermalizes in a state that is neither  $i$  nor  $j$ . Thus, a better estimate of the transition rate constant can be obtained as  $k_{i \rightarrow j} = f_{d,ij} k_{i \rightarrow j}^{\text{TST}}$ , where the dynamical correction factor (transmission coefficient)  $f_{d,ij}$  expresses the ratio of successful trajectories over total trajectories through the bottleneck surface (see Figure 9b). An excellent estimate of  $f_{d,ij}$  can be obtained at modest computational cost via short MD runs (see ref 4) initiated at the bottleneck, which thermalize quickly in a state.<sup>63,64</sup>

Once one has the network of states and the interstate transition rate constants  $k_{i \rightarrow j}$  (see Figure 8), one can solve the master equation (eq 11) analytically for the time-dependent probabilities of occupancy of the states.<sup>65</sup> In many cases, however, it is more convenient to generate stochastic trajectories consisting of long sequences of elementary transitions (jumps) between states. An ensemble of such stochastic trajectories essentially constitutes

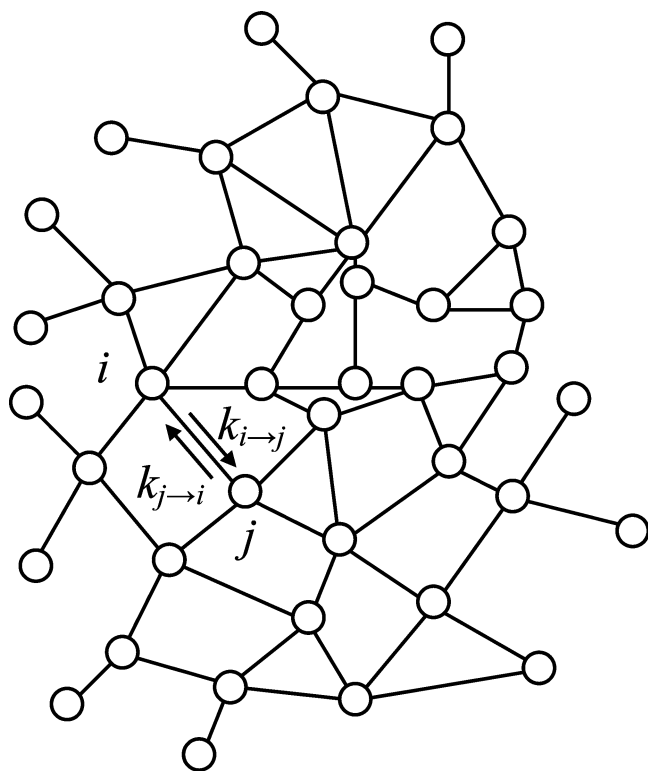


**Figure 8.** Schematic of a system evolving through infrequent transitions between states. Each state  $i$  is a low-energy region in configuration space (basin of the energy hypersurface) surrounded by energy barriers. The mean residence time in a state is long, in comparison to the relaxation time required for the system in order to reach a stationary distribution among configurations in the state. Transitions between states  $i$  and  $j$  are described by rate constants  $k_{i \rightarrow j}$  and  $k_{j \rightarrow i}$ . These are related to the equilibrium probabilities of occupancy of the states,  $P_i^{\text{eq}}$  and  $P_j^{\text{eq}}$ , through the condition of detailed balance,  $k_{i \rightarrow j} P_i^{\text{eq}} = k_{j \rightarrow i} P_j^{\text{eq}}$ .

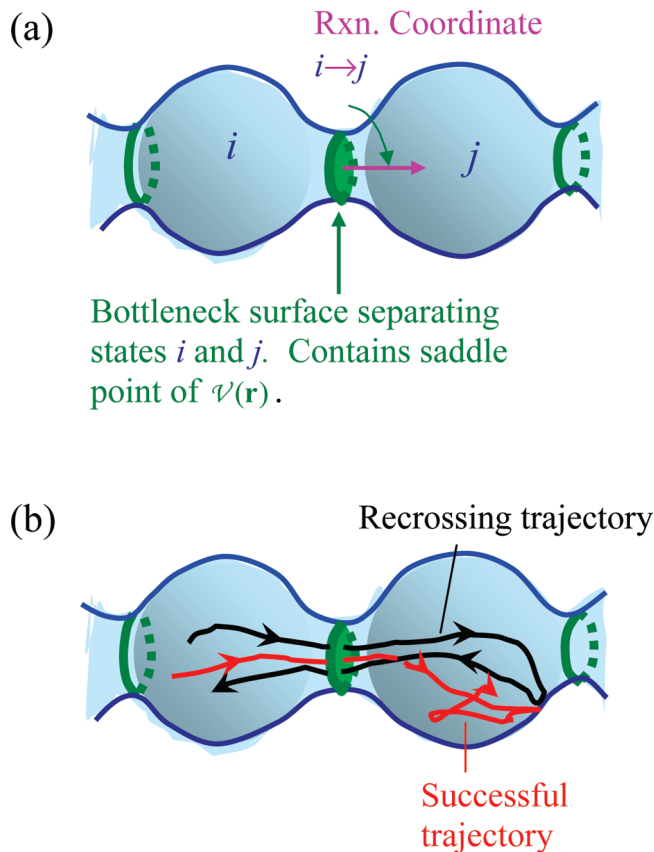


**Figure 9.** (a) Simple geometric representation of states and dividing surface in the case of a system with three degrees of freedom. The blue envelope is an equipotential surface. Each state contains a local minimum of the potential energy. The dividing (bottleneck) surface, shown in green, goes through a saddle point of the potential energy and is everywhere tangent to the gradient vector of the potential energy. At the dividing surface, the “reaction coordinate” is directed along the eigenvector corresponding to the negative eigenvalue of the Hessian matrix of second derivatives of the energy. (b) Examples of a successful dynamical trajectory and a recrossing trajectory in the simple three-dimensional system.

a numerical solution of the master equation (eq 11), subject to given initial conditions. Kinetic Monte Carlo (KMC) simulation is a method used for the generation of such stochastic trajectories. It is based on the realization that a succession of independent elementary transitions, such as those considered in the theory of infrequent events, constitutes a Poisson process.

Assume that the stochastic trajectory finds itself in state  $i$  at time  $t$ . To sample the next transition, the KMC method computes the total rate constant for leaving state  $i$ ,  $k_{i \rightarrow} = \sum_j k_{i \rightarrow j}$ . It then chooses a time interval for leaving state  $i$  as  $\Delta t = -(\ln(1 - \xi))/k_{i \rightarrow}$ , where  $\xi \in [0,1)$  is a uniformly distributed pseudo-random number. The state  $j$  to which a transition will occur is chosen among all states connected to state  $i$ , according to the probabilities  $k_{i \rightarrow j}/k_{i \rightarrow}$ . The time is incremented by  $\Delta t$ , the current state of the system is updated to  $j$ , and the algorithm loops back to sample the next transition.

The KMC method has found widespread use in sampling dynamical processes that occur as successions of uncorrelated elementary transitions. An early chemical engineering application can be found in the work of June et al.<sup>64</sup> on diffusion in zeolites. Long stochastic trajectories  $\mathbf{r}(t)$  for a sorbed molecule were generated as sequences of transitions between positions (sorption sites) derived from energy minima in the zeolite channels and the self-diffusion coefficient was obtained through the Einstein relation:

$$D_s = \lim_{t \rightarrow \infty} \frac{\langle [\mathbf{r}(t) - \mathbf{r}(0)]^2 \rangle}{6t} \quad (14)$$

For xenon in silicalite, an analysis of the potential energy hypersurface reveals three sorption sites, corresponding to the sorbed molecule residing in a straight-channel segment, in a sinusoidal channel segment, or in a channel intersection.<sup>64</sup> Values of the self-diffusivity at low occupancy,  $D_s$ , predicted at three different temperatures by estimating rate constants for interstate transitions and then using these rate constants within long KMC simulations, are shown in Table 1.  $D_s$  values obtained by direct MD simulation are given in the same table; these constitute “exact” results for the potential energy model employed and are in excellent agreement with pulsed-field-gradient NMR measurements by Kärger et al.<sup>66</sup> No value based on  $D_s$  at 100 K is provided in the MD column of Table 1, because, at the time of the calculation, diffusion at this temperature was too slow to be predicted reliably by MD. We see that the infrequent-event analysis gives estimates for the self-diffusivity and its activation energy that are in very favorable agreement with the full MD calculation, in a small fraction of the CPU time. In more complex problems involving cascades of jumps in multidimensional configuration spaces,<sup>65</sup> MD is extremely limited in terms of the time scales that it can address; infrequent event analysis is the only way that one can learn about the long-time dynamics, which governs properties in applications.

## 9. Conclusions and Outlook

In the 56 years since its invention, the Monte Carlo (MC) method has developed into a powerful set of computational techniques for understanding and predicting the equilibrium and dynamical properties of physical, chemical, materials, and biological systems.

The MC methodology is extremely versatile. New techniques and algorithms can enhance efficiency of sampling complex configuration spaces by orders of magnitude. Combination of different techniques boosts numerical performance. Through MC sampling and kinetic MC methods, long-time dynamics can be made accessible in systems evolving through infrequent transitions in a network of states.

In the last 25 years, chemical engineers have played a prominent role in devising new ensembles, moves, and algorithms for conducting MC simulations and improving existing ones. Some very difficult scientific and engineering problems have been solved, thanks to their efforts. Several MC methods developed by chemical engineers have constituted breakthroughs for the entire molecular simulation community.

Where should one use MC methodology, rather than any other type of particle-based simulation method to predict the properties of matter? One can think of several types of problems where the MC method offers distinct advantages:

(i) *Problems requiring the prediction of fluid-phase equilibria (vapor–liquid equilibria, liquid–liquid equilibria, sorption equilibria in microporous solids, aggregation versus phase separation in solutions of amphiphiles) from molecular-level structure and interactions.* Molecular insertion and deletion moves for estimating chemical potentials or equalizing chemical potentials between phases, and special sampling techniques for improving the performance of such moves (in the case of bulky molecules or molecules of complex shape) are easier to implement in a MC methodology, rather than in a MD simulation framework.

(ii) *Problems requiring the calculation of a free energy, with respect to a coarse-grained variable (order parameter) that cannot be easily incorporated in an effective potential to bias the dynamical equations of motion.* A variety of nucleation

**Table 1. Low-Temperature Diffusion of Xenon in Silicalite-1, as Predicted by MC Integration and KMC-Based Infrequent Event Analysis and by MD Simulation<sup>64</sup>**

parameter	dynamically corrected transition-state theory, TST	molecular dynamics, MD <sup>a</sup>
self-diffusivity, $D_s$ ( $10^{-4}$ cm <sup>2</sup> /s)		
at 100 K	0.046	
at 200 K	0.44	0.51
at 300 K	1.11	1.5
activation energy for diffusion (kJ/mol)	5.2	5.5
relative CPU time	1	10

<sup>a</sup> In excellent agreement with the pulsed-field-gradient NMR measurements of Kärger et al.<sup>66</sup>

problems fall in this category (for example, nucleation of a vapor phase within a liquid, where the density has been used within umbrella sampling schemes to derive the Gibbs energy as a function of cavity size,<sup>67</sup> or nucleation of a solid phase from the liquid, where the number of molecules constituting a crystal nucleus has been employed as an order parameter<sup>68</sup>).

(iii) *Problems involving long-chain, entangled polymers (e.g., in bulk melts, at interfaces, or as matrices in nanocomposites), or even short-chain molecules in confined geometries (e.g., in sorption equilibria of chain molecules in zeolites and other microporous solids).* The rate of equilibration afforded by connectivity-altering and configurational bias Monte Carlo (CBMC) moves is several orders of magnitude faster than that which can be achieved by molecular dynamics (MD). Even when one is interested in dynamics, MC strategies that allow the calculation of energy and entropy as functions of a set of slowly evolving variables (e.g., of the conformation tensor in unentangled melts<sup>69</sup>) or mapping onto entanglement networks,<sup>70</sup> whose evolution can be simulated through slip-link models<sup>71</sup> in entangled melts, may be superior to equilibrium or nonequilibrium MD simulation for probing constitutive relations and accessing deformation rates comparable to those encountered in processing operations.

(iv) *Problems involving the assessment of environmental effects on the equilibrium composition and properties of chemically reacting systems.* Reaction ensemble MC methods,<sup>19</sup> invoking a minimal set of ideal gas-state thermochemical data, can converge to chemical equilibrium much more quickly than more fundamental approaches tracking the actual reaction mechanisms, such as *ab initio* MD or quantum mechanics/molecular mechanics (QM/MM) methods.

What is the future of MC methods? One can clearly discern an ever-expanding range of applicability of the MC methodology. The properties and phase equilibria of polymers, colloids, proteins, biological membranes, liquid crystals, semiconductors, interfaces, nanocomposites, nanostructured materials for energy production and storage, ionic liquids and other “green” solvents are just a few examples of areas in which chemical engineers and other scientists are pushing the frontiers of molecular-based understanding and prediction.

Recently, we have witnessed increased use of the MC methodology as part of multiscale modeling and simulation schemes for accessing long length-scale and time-scale phenomena: coarse-graining of atomistic into mesoscopic representations, sampling of molecular configurations in field theoretic approaches, computation of transition rate constants, and generation of stochastic trajectories for processes occurring as long sequences of infrequent events are just a few examples.

One also sees fertile interactions developing between molecular simulators and “systems” (process design and optimiza-

tion) researchers. There is very much to be gained if these communities join forces to address complex process and product design problems with the help of MC simulations.

## Acknowledgment

Support from the Senate Committee on Basic Research of the National Technical University of Athens, in the form of a PEVE 2006 "Karathéodory" program, is gratefully acknowledged.

## Literature Cited

- (1) Metropolis, N.; Rosenbluth, A. W.; Rosenbluth, M. N.; Teller, A. H.; Teller, E. *J. Chem. Phys.* **1953**, *21*, 1087.
- (2) Allen, M. P.; Tildesley, D. J. *Molecular Simulation of Liquids*; Clarendon: Oxford, 1987.
- (3) Frenkel, D.; Smit, B. *Understanding Molecular Simulation: From Algorithms to Applications*, 2nd Edition; Academic Press: San Diego, CA, 2002.
- (4) Elliott, J. R.; Maginn, E. J. Historical Perspective and Current Outlook for Molecular Dynamics as a Chemical Engineering Tool. *Ind. Eng. Chem. Res.* **2010**, *49*, DOI: 10.1021/ie901898k.
- (5) Dickman, R.; Hall, C. K. *J. Chem. Phys.* **1988**, *89*, 3168.
- (6) Müller, E. A.; Gubbins, K. E. *Ind. Eng. Chem. Res.* **2001**, *40*, 2193.
- (7) Gubbins, K. E.; Moore, J. D. Molecular Modeling of Matter: Impact and Prospects in Engineering. *Ind. Eng. Chem. Res.* **2010**, *49*, DOI: 10.1021/ie901909c.
- (8) Peterson, B. K.; Gubbins, K. E. *Mol. Phys.* **1987**, *62*, 215.
- (9) Evans, R.; Marini Bettolo Marconi, U.; Tarazona, P. *J. Chem. Phys.* **1986**, *84*, 2376.
- (10) Panagiotopoulos, A. Z. *Mol. Phys.* **1987**, *61*, 813.
- (11) Panagiotopoulos, A. Z. In *Simulation Methods for Polymers*; Kotlyanskii, M., Theodorou, D. N., Eds.; Marcel Dekker: New York, 2004; Chapter 9.
- (12) Kofke, D. A. *Adv. Chem. Phys.* **1998**, *105*, 405.
- (13) Theodorou, D. N. In *Materials Science of Membranes for Gas and Vapor Separation*; Yampolskii, Yu., Pinnau, I., Freeman, B. D., Eds.; John Wiley: Hoboken, NJ, 2006; pp 47–92.
- (14) Briano, J. G.; Glandt, E. D. *J. Chem. Phys.* **1984**, *80*, 3336.
- (15) Kofke, D. A.; Glandt, E. D. *Mol. Phys.* **1988**, *64*, 1105.
- (16) Pant, P. V. K.; Theodorou, D. N. *Macromolecules* **1995**, *28*, 7224.
- (17) Johnson, J. K.; Panagiotopoulos, A. Z.; Gubbins, K. E. *Mol. Phys.* **1994**, *81*, 717.
- (18) Smith, W. R.; Trřska, B. *J. Chem. Phys.* **1994**, *100*, 3019.
- (19) Turner, H. C.; Brennan, J. K.; Lřsal, M.; Smith, W. R.; Johnson, J. K.; Gubbins, K. E. *Mol. Simul.* **2008**, *34*, 119.
- (20) Turner, H. C.; Brennan, J. K.; Johnson, J. K.; Gubbins, K. E. *J. Chem. Phys.* **2002**, *116*, 2138.
- (21) Lyubartsev, A. P.; Martinovski, A. A.; Shevkunov, S. V.; Vorontsov-Yelyaminov, P. N. *J. Chem. Phys.* **1991**, *96*, 1776.
- (22) De Pablo, J. J.; Escobedo, F. A. *J. Chem. Phys.* **1996**, *105*, 4391.
- (23) de Pablo, J. J.; Yan, Q.; Escobedo, F. A. *Annu. Rev. Phys. Chem.* **1999**, *50*, 377.
- (24) Yan, Q. L.; de Pablo, J. J. *J. Chem. Phys.* **2000**, *113*, 1276.
- (25) De Pablo, J. J. In *Simulation Methods for Polymers*; Kotlyanskii, M., Theodorou, D. N., Eds.; Marcel Dekker: New York, 2004; Chapter 7.
- (26) Swendsen, R. H.; Wang, J.-S. *Phys. Rev. Lett.* **1986**, *57*, 2607.
- (27) Geyer, C. J. In *Computing Science and Statistics: Proceedings of the 23rd Symposium on the Interface*; American Statistical Association: New York, 1991; p 156.
- (28) Earl, D. J.; Deem, M. W. *Phys. Chem. Chem. Phys.* **2005**, *7*, 3910.
- (29) Falcioni, M.; Deem, M. W. *J. Chem. Phys.* **1999**, *110*, 1754.
- (30) Rosenbluth, M. N.; Rosenbluth, A. W. *J. Chem. Phys.* **1955**, *23*, 356.
- (31) Siepmann, J. I.; Frenkel, D. *Mol. Phys.* **1992**, *75*, 59.
- (32) De Pablo, J. J.; Laso, M.; Suter, U. W. *J. Chem. Phys.* **1992**, *96*, 2395.
- (33) Dodd, L. R.; Boone, T. D.; Theodorou, D. N. *Mol. Phys.* **1993**, *78*, 961.
- (34) Mavrantzas, V. G.; Boone, T. D.; Zervopoulou, E.; Theodorou, D. N. *Macromolecules* **1999**, *32*, 5072.
- (35) Wu, M. G.; Deem, M. W. *J. Chem. Phys.* **1999**, *111*, 6625.
- (36) Note, however, that millisecond-long MD simulations on specialized hardware have been reported recently. For a brief discussion and references, see ref 4.
- (37) Theodorou, D. N. In *Bridging Time Scales: Molecular Simulations for the Next Decade*; Nielaba, P., Mareschal, M., Ciccotti, G., Eds.; Springer-Verlag: Berlin, 2002; pp 69–128.
- (38) (a) Karayiannis, N. Ch.; Mavrantzas, V. G.; Theodorou, D. N. *Phys. Rev. Lett.* **2002**, *88*, 105503. (b) Karayiannis, N. Ch.; Giannousaki, A. E.; Mavrantzas, V. G.; Theodorou, D. N. *J. Chem. Phys.* **2002**, *117*, 5465.
- (39) Theodorou, D. N. *Chem. Eng. Sci.* **2007**, *62*, 5697.
- (40) Ramos, F. J.; Peristeras, L.; Theodorou, D. N. *Macromolecules* **2007**, *40*, 9640.
- (41) Kofke, D. A. *Fluid Phase Equilib.* **2005**, *228–229*, 41.
- (42) Jarzynski, C. *Phys. Rev. Lett.* **1997**, *78*, 2690.
- (43) (a) Widom, B. *J. Chem. Phys.* **1963**, *39*, 2808. (b) Widom, B. *J. Phys. Chem.* **1982**, *86*, 869.
- (44) Maginn, E. J.; Bell, A. T.; Theodorou, D. N. *J. Phys. Chem.* **1995**, *99*, 2057.
- (45) Boulougouris, G. C.; Economou, I. G.; Theodorou, D. N. *Mol. Phys.* **1999**, *96*, 905.
- (46) Theodorou, D. N. *J. Chem. Phys.* **2006**, *124*, 034109.
- (47) Shi, W.; Maginn, E. J. *J. Chem. Theory Comput.* **2007**, *3*, 1451.
- (48) Maginn, E. J. *Acc. Chem. Res.* **2007**, *40*, 1200.
- (49) Maginn, E. J.; Bell, A. T.; Theodorou, D. N. *J. Phys. Chem.* **1996**, *100*, 7155.
- (50) Jobic, H.; Theodorou, D. N. *Microporous Mesoporous Mater.* **2007**, *102*, 21.
- (51) Mavrantzas, V. G.; Theodorou, D. N. *Macromolecules* **1998**, *31*, 6310.
- (52) (a) Kofke, D. A. *Mol. Phys.* **1993**, *78*, 1331. (b) Kofke, D. A. *J. Chem. Phys.* **1993**, *98*, 4149.
- (53) Bruce, A. D.; Wilding, N. B. *Phys. Rev. Lett.* **1992**, *68*, 193.
- (54) Orkoulas, G.; Panagiotopoulos, A. Z. *J. Chem. Phys.* **1999**, *110*, 1581.
- (55) Ferrenberg, A. M.; Swendsen, R. H. *Phys. Rev. Lett.* **1989**, *63*, 1195.
- (56) Panagiotopoulos, A. Z.; Wong, V.; Floriano, M. A. *Macromolecules* **1998**, *31*, 912.
- (57) Smith, G. R.; Bruce, A. D. *J. Phys. A* **1995**, *28*, 6623–6643. Wang, J.-S.; Tay, T. K.; Swendsen, R. H. *Phys. Rev. Lett.* **1999**, *82*, 476.
- (58) (a) Errington, J. R. *J. Chem. Phys.* **2003**, *118*, 9915. (b) Errington, J. R. *J. Chem. Phys.* **2003**, *119*, 3405. (c) Paluch, A. S.; Shen, V. K.; Errington, J. R. *Ind. Eng. Chem. Res.* **2008**, *47*, 4533.
- (59) Wang, F.; Landau, D. P. *Phys. Rev. Lett.* **2001**, *86*, 2050.
- (60) Shell, M. S.; Debenedetti, P. G.; Panagiotopoulos, A. Z. *J. Chem. Phys.* **2003**, *119*, 9406.
- (61) Mastny, E. A.; de Pablo, J. J. *J. Chem. Phys.* **2005**, *112*, 124109.
- (62) Rathore, N.; Knotts, T. A.; de Pablo, J. J. *Biophys. J.* **2006**, *90*, 1767.
- (63) (a) Chandler, D. *J. Chem. Phys.* **1978**, *68*, 2959. (b) Voter, A. F.; Doll, J. D. *J. Chem. Phys.* **1985**, *82*, 80.
- (64) June, R. L.; Bell, A. T.; Theodorou, D. N. *J. Phys. Chem.* **1991**, *95*, 8866.
- (65) Boulougouris, G. C.; Theodorou, D. N. *J. Chem. Phys.* **2009**, *130*, 044905.
- (66) Heink, W.; Křrger, J.; Pfeifer, H.; Stallmach, F. *J. Am. Chem. Soc.* **1990**, *112*, 2175.
- (67) Shen, V. K.; Debenedetti, P. G. *J. Chem. Phys.* **1999**, *111*, 3581.
- (68) Yi, P.; Rutledge, G. *J. Chem. Phys.* **2009**, in press.
- (69) Ilg, P.; Öttinger, H. C.; Kröger, M. *Phys. Rev. E* **2009**, *79*, 011802.
- (70) Tzoumanekas, C.; Theodorou, D. N. *Macromolecules* **2006**, *39*, 4592.
- (71) Masubuchi, Y.; Takimoto, J.-I.; Koyama, K.; Ianniruberto, G.; Marrucci, G.; Greco, F. *J. Chem. Phys.* **2001**, *115*, 4387.

**Doros N. Theodorou\***

*Department of Materials Science and Engineering, School of Chemical Engineering, National Technical University of Athens, 9 Heroon Polytechniou Street, Zografou Campus, Athens 15780, Greece*

Received for review December 2, 2009

IE9019006